Direct Heuristic Dynamic Programming for Damping Oscillations in a Large Power System

Chao Lu, *Member, IEEE*, Jennie Si, *Fellow, IEEE*, and Xiaorong Xie, *Member, IEEE*

Abstract—This paper applies a neural-network-based approximate dynamic programming method, namely, the direct heuristic dynamic programming (direct HDP), to a large power system stability control problem. The direct HDP is a learning- and approximation-based approach to addressing nonlinear coordinated control under uncertainty. One of the major design parameters, the controller learning objective function, is formulated to directly account for network-wide low-frequency oscillation with the presence of nonlinearity, uncertainty, and coupling effect among system components. Results include a novel learning control structure based on the direct HDP with applications to two power system problems. The first case involves static var compensator supplementary damping control, which is used to provide a comprehensive evaluation of the learning control performance. The second case aims at addressing a difficult complex system challenge by providing a new solution to a large interconnected power network oscillation damping control problem that frequently occurs in the China Southern Power Grid.

Index Terms—Approximate dynamic programming (ADP), direct heuristic dynamic programming (direct HDP), neural networks, power system stability control.

I. INTRODUCTION

A POWER system is a complex network composed of many different components such as generators, ac or dc transmission lines, and various types of load. The most important task of power system control is to maintain stable operation of the system. Exciter and governor control of generators are traditional approaches to power system stability. High-voltage direct current (HVDC) and flexible ac transmission system (FACTS) devices are modern control techniques that are frequently adopted in recent years. However, system nonlinearity, uncertainty, and coordinated control among multiple controllers remain three major challenges for controller design in such extra-large-scale systems.

Many nonlinear phenomena are apparent in a power system, including dead zone and control limits to name a few. In addition, some special characteristics of nonlinear systems, bifurcation, and chaos, for example, have also been observed in power systems [1]. The system uncertainty usually comes from deviations in system models and parameters, and the frequently

C. Lu and X. Xie are with the Department of Electrical Engineering, Tsinghua University, Beijing 100084, China (e-mail: luchao @tsinghua.edu.cn).

J. Si is with the Department of Electrical Engineering, Arizona State University, Tempe, AZ 85287 USA (e-mail: si@asu.edu).

changing power system operating conditions [2]. Advances in power electronics have made power systems more controllable. For some global stability problems such as low-frequency oscillation at a network level, it is essential that coordination among various control devices is considered. However, most current controllers are designed and tuned independently.

To solve the above problems, some advanced control techniques have been applied in power system control, such as linearization [3], energy function method [4], robust control [5], adaptive control [6], and multiple-input–multiple-output (MIMO) design [7]. However, most of these are based on accurate models usually not available in real complex systems. In addition, there is no systematic procedure that simultaneously takes into account complex nonlinear dynamics and system uncertainties for a coordinated controller design to address large power network stability. This paper attempts that goal by using an approximate dynamic programming (ADP) method in the China Southern Power Grid (CSG) as an example.

Several ADP methods have been attempted to address power system problems. A generator control using dual heuristic programming (DHP) was implemented via digital simulations and physical experiments [8]. In [9], supplementary damping control of FACTS devices was studied using test systems with no more than ten generators.

In this paper, we consider the application of a model-independent ADP approach to coordinated wide-area low-frequency oscillation damping control. This method was initially proposed in [10] and is now referred to as the direct heuristic dynamic programming (direct HDP). It is a design inspired by Werbos' ADHDP. The term "direct" is adopted from the adaptive control literature where "direct adaptive control" corresponds to the adaptive architecture that no plant parameter estimation takes place, but instead, plant information is used to find controller parameters directly. In [11], [12], the direct HDP was embedded to stabilization and tracking control of an Apache helicopter using a full-scale industrial Apache model. This is a complex continuous-state/control MIMO nonlinear system with uncertainty. These results suggest the potential of direct HDP for scalable complex system control applications. Additionally, for the low-frequency-oscillation problem in multimachine power systems under consideration, the swing period is usually greater than 1 s. Therefore, the controller has sufficient time to learn and adapt. This motivates the idea of using direct HDP to address nonlinearity, uncertainty, and coordination among multiple system components.

In this paper, we first examine the case of a classic four-machine two-area (4M2A) system [13], in which the learning and generalization abilities of a static var compensator (SVC) supplementary controller in a nonlinear and uncertain environment are validated. The other case considers CSG,
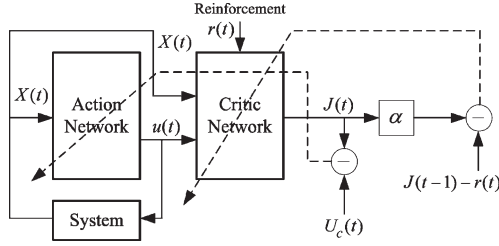
Fig. 1. Schematic for implementation of the direct HDP.

which includes 2329 buses, 335 generators, and 1254 load counts. Modulation controllers for two parallel HVDC links are designed such that coordination between them can be achieved.

II. FRAMEWORK OF DIRECT HDP CONTROL

For a real power grid, real-time power system dynamics are provided by a wide-area measurement system (WAMS), which is based on synchronized phasor measurement techniques and modern digital communication networks. Through this system, key system variables such as internal voltage angles of the generators in different areas, which were not available in the past, can now be measured directly and used as feedback to improve global system performance [14].

During the offline design, system responses are produced based on the time-domain simulation of various power system components, which can be described by a set of algebraic differential equations. The following equation represents one simple generator model:

$$\begin{cases} u_d = x_q i_q - r i_d, \quad u_q = E_q - x_d i_d - r i_d \\ E'_q = E_q - (x_d - x'_d)\, i_d, \quad M_e = (i_d u_d + i_q u_q)/\omega \\ dE'_q/dt = (E_{fd} - E_q)/T'_{d0} \\ d\Delta\omega/dt = (M_m - M_e - D)/T_J \\ d\delta/dt = \omega_0(\omega - 1). \end{cases} \quad (1)$$

The descriptions and notations used in (1) can be found in [13].

Employing other dynamic devices such as excitation control, speed governor, motor, and FACTS greatly increases the system order, and the network connections through lines and transformers enhance the coupling effect. It is common that a power system has more than ten thousand state variables.

A direct HDP controller that was first introduced in [10] is briefly summarized below to provide a notational convention for ease of further discussion. It comprises two main parts: 1) an action network and 2) a critic network. The former produces control signals according to the learned policy, whereas the latter approximates the function J of the Bellman equation in dynamic programming. Fig. 1 is the schematic diagram [10].

The output of the critic network (the J function) approximates the discounted total cost-to-go. Specifically, it approximates $R(t)$, which is given by $\sum_{k=1}^{\infty} \alpha^{k-1} r(t+k)$, where $R(t)$ is the future accumulative cost-to-go value at time t, and α is a discount factor for the infinite-horizon problem $(0 < \alpha < 1)$. The critic network is trained to approximate the "value function" $J(t)$ by minimizing the objective function, i.e., $E_c(t) = 0.5e_c(t)^2$, where $e_c(t) = \alpha J(t) - [J(t-1) - r(t)]$. The principle behind adapting the action network is the back-propagation of the error between the desired ultimate objective,

which is denoted by U_c, and the cost function $R(t)$. In this paper, for notational simplicity, $J(t)$ represents either the actual or the approximate cost function, depending on the context.

In this direct HDP approach, the cost function is the only feedback to the controller on its performance. For the power system control problems under consideration, interarea oscillation is an interactive process among generator groups in different regions. The average rotor speed deviation of the generators is a physically feasible and appropriate reflection on such low-frequency oscillations. In this paper, the reinforcement signal $r(t)$ is formulated as

$$r(t) = -\left(\sum_{i=1}^{m} b_i \Delta\omega_{\text{inter}-i}^2 + \sum_{j=1}^{n} b_{m+j} \Delta\omega_{\text{local}-j}^2 \right) \quad (2)$$

where $\Delta\omega_{\text{inter}-i}$ and $\Delta\omega_{\text{local}-j}$ are the rotor speed deviation corresponding to the ith interarea and the jth local modes, respectively, which represent the overall degree of oscillation. Additionally, in the equation, b_i $(i = 1, 2, \ldots, m + n)$ are the weights on different modes. By adjusting these weights, the oscillation mode that is detrimental to system stability is chosen to be suppressed with high priority. During normal operation, all generators are synchronized, and all the rotor speed deviations are equal to zero. Since all designed controllers utilize the same cost function as shown in (2), the overall cost cannot be optimal if only some of the oscillation modes are damped partially. Therefore, minimization of the cost function is a good indicator of the level of coordinated control among different oscillation modes. In addition, $X(t)$ denotes selected system states, and $u(t)$ is the supplementary damping control signal used in the power system stabilization considered herein.

In this paper, the action and critic networks are implemented using multilayer perceptron (MLP) neural networks (NNs) with one hidden layer. The number of network inputs and outputs corresponds with the control problem at hand. In this paper, without systematic validation and optimization, six hidden layer neurons are used. This control structure can easily be extended to MIMO cases. The learning algorithm was adopted from [10], which is based on gradient descent.

The action and the critic network learning is carried out within a task–run–trial framework. Specifically, a task signifies learning under one consistent power system condition, including the same disturbance settings. A task includes many runs. Each run begins with a new random initialization of the action and critic network parameters. A trial is a simulation of the power system dynamics, given the controller parameter setting, an initial system operating point, and some designed disturbances. If the controller fails to stabilize the system in one trial, another trial is carried out based on the network weights saved from the previous trial, until the damping ratio of the oscillation in one trial is greater than 5%. At that point, the run is considered successful. Otherwise, if the allowable maximum trial number is reached, this run is considered a failure. Since the learning controller parameter initialization is random and the system dynamics are nonlinear, there exist multiple local minima in the error surface. The resulting controllers from different successful trials are not guaranteed to be identical. Typically, a controller that resulted from a high damping ratio is adopted. In addition, the system instability criterion is the
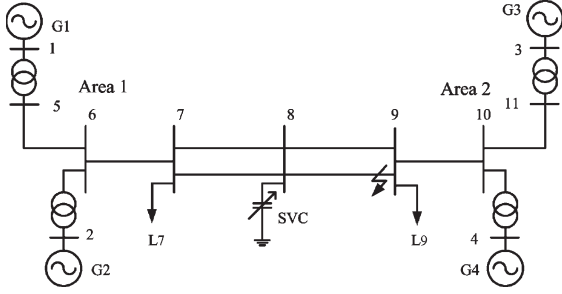
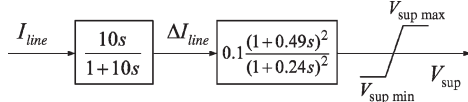Fig. 2. Single-line diagram of the two-area test system.

Fig. 3. Block diagram of the conventional supplementary controller.

maximal generator power angle difference $\Delta\delta$. It is impossible for $\Delta\delta$ to exceed 180° in practical stable power systems.

III. SVC SUPPLEMENTARY CONTROL OF A 4M2A SYSTEM

The learning ability of the direct HDP controller is first demonstrated using a benchmark 4M2A system [13], as shown in Fig. 2, to study the power system oscillation problem. There are three oscillation modes in this system: two are local, and one is interarea. The frequency of the interarea mode is 0.55 Hz.

An SVC is placed at the center of the tie lines to maintain voltage stability and suppress swings. The traditional PID controller is evaluated first. However, this method alone cannot guarantee system stability under serious faults. Therefore, supplementary control is needed. In [13], this controller design is based on the conventional pole-placement method, whose block diagram is shown in Fig. 3, where V_{sup} is the output of this supplementary controller, $V_{\text{supmax}} = -V_{\text{supmin}} = 0.1$ pu. The input signal I_{line} is the magnitude of the current in the line between buses 9 and 10, and ΔI_{line} is the oscillation signal after the washout block.

A. Direct HDP Control in 4M2A System

To compare control performances of the direct HDP and conventional controllers, the same input signal I_{line} is used. The phase adjustment of the supplementary control input ΔI_{line} is critical to damping the oscillations, which is implemented by the two phase-shift blocks in a conventional approach (see Fig. 3). However, if only ΔI_{line} is used as the input, an ordinary MLP NN with a small number of hidden nodes is not capable of changing the phase values of ΔI_{line} sufficiently to suppress the swing. To address this issue, an additional input $d\Delta I_{\text{line}}/dt$, i.e., the derivative of ΔI_{line}, is necessary, with an approximate implementation shown in Fig. 4. The gains are adjusted to scale the neural network inputs between -1 and 1. The control limits are the same as those in Fig. 3.

For the 4M2A system, the reinforcement $r(t)$ is

$$r(t) = -\left(b_1 \Delta\omega_{\text{interarea}}^2 + b_2 \Delta\omega_{\text{local-1}}^2 + b_3 \Delta\omega_{\text{local-2}}^2\right) \quad (3)$$
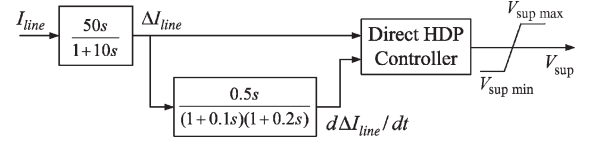
Fig. 4. Block diagrams of supplementary controllers using the direct HDP method.

where $\Delta\omega_{\text{interarea}} = ((\omega_1+\omega_2) - (\omega_3+\omega_4))/2$, $\Delta\omega_{\text{local-1}} = \omega_1 - \omega_2$, and $\Delta\omega_{\text{local-2}} = \omega_3 - \omega_4$, and ω_i $(i = 1, 2, 3, 4)$ is the rotor speed of the ith generator.

B. Learning From Random Initialization

In this section, the 4M2A system is used to study the learning capability of direct HDP controller. The basic problem setting is that a three-phase short circuit occurs near bus 9 and is cleared by tripping the line between buses 8 and 9 after 74 ms. This case is used to train the direct HDP controller from random initialization. Here is a typical learning process that includes two trials as described below. In trial 1, since the initialization was random, control output directions during the first several seconds were not in accordance with the desired actions. The system was destabilized after 4 s, and simulation was terminated upon reaching the failure criterion. However, this trial, which is characterized by a failure, provided the direct HDP controller a considerable amount of useful information about which state–action pairs may have brought instability and should therefore be avoided. This trial constitutes the basis of performance improvement in the next trial. In trial 2, refined and accurate control strategies were obtained. After faults, the output of the controller switches between the upper and lower bounds in order to fully utilize the control power. For reduced oscillations, the control magnitude also decreases accordingly such that the system can reach a steady state quickly. Additional training based on trial 2 can increase the speed of controller response further.

Controller performances of the two different approaches are further compared. The results indicate that the direct HDP controller achieves a slightly better performance than the specially designed traditional controller.

C. Generalization and Adaptation of the Direct HDP

In order to test the controller performances under different operating conditions, the following scenarios were created.

Case 1: The system structure and load flow were the same as in the basic case, but a short-circuit fault occurred near bus 8 on one line between buses 7 and 8. This fault was cleared by line tripping after 74 ms.

Case 2: The load at bus 9 was reduced from 1769 to 1569 MW, and correspondingly, an active power of 200 MW injected into the network from generator 2 was reduced. The disturbance setting was the same as in the basic case.

Case 3: Similar to case 2, except that the line between buses 7 and 8 was out of service and no line tripping occurred after the instantaneous short-circuit fault.

In Cases 1 and 2, the weights of action and critic networks in the direct HDP controller were fixed after learning was declared successful. Results are shown in Fig. 5.
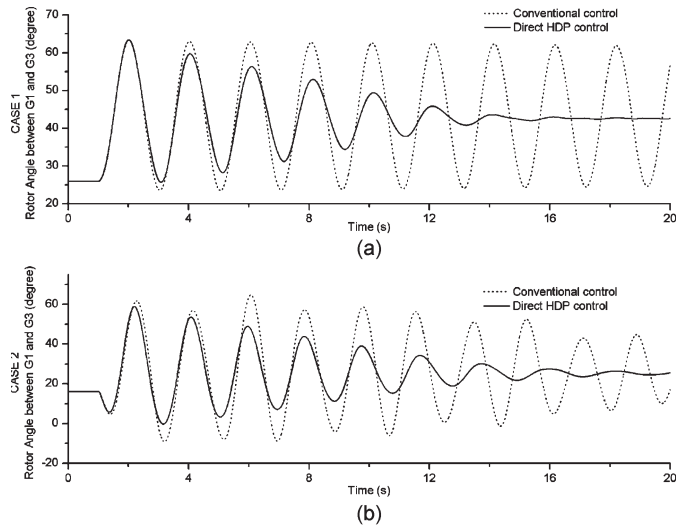
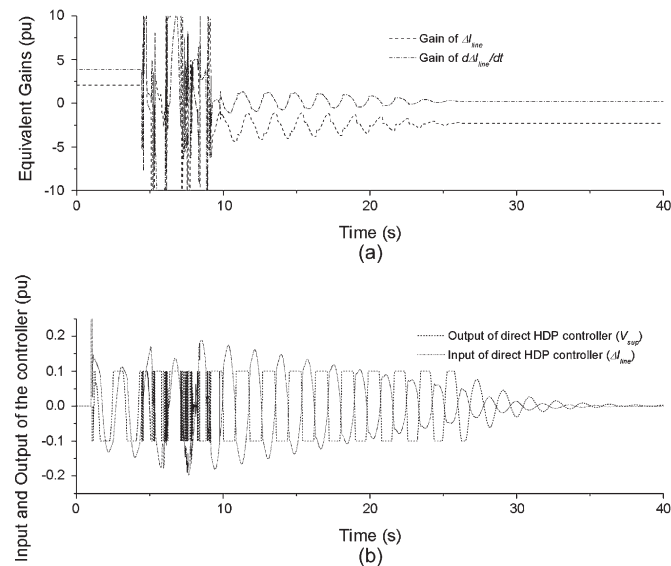Fig. 5. Rotor angle between G1 and G3 under different system conditions.

Fig. 6. Online learning performances of the direct HDP controller.
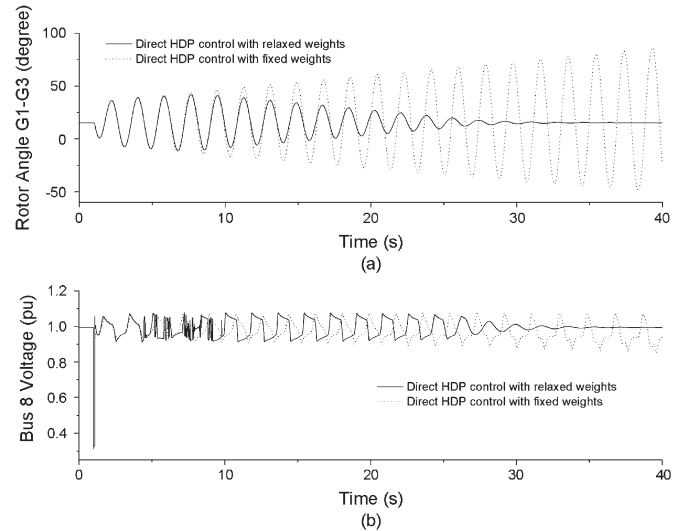

Fig. 7. Learning process when the system configurations change significantly.

Fig. 8. AC/DC parallel structure of the power transmission in CSG.

In the beginning, the equivalent gains of the two input signals related to I_{line} were positive, but upon completion of learning, the gains became negative [Fig. 6(a)]. This is shown more clearly in the phase relationship between the input signal ΔI_{line} and the output signal V_{sup}, which changes from nearly the same phase during the first 5 s to a nearly reversed phase after 10 s through online learning [Fig. 6(b)]. The new control policy damps the oscillations well (Fig. 7).

IV. HVDC POWER CONTROL USING DIRECT HDP FOR CSG

CSG is an ac/dc hybrid power system and is mainly composed of four provincial grids (Fig. 8). The transmission distance from the west to the east is over 1000 km. The large capacity of power transmission takes place through six 500-kV ac lines and two HVDC links (Gaozhao and Tianguang) in parallel in 2006. This paper is based on the 2006 network data and geometry. Low-frequency oscillations have become a prominent problem and created potential threats to the system stability. In this situation, the power modulation control using HVDC is an attractive alternative, given its huge adjustable capacity and its fast responding characteristics. The structure of a conventional modulation controller is similar to that in Fig. 3. However, the multiple HVDC modulation controllers are usually designed independently. Coordination of the controllers is a challenging issue and has not been addressed. It is attempted in this paper by using the direct HDP method.

These results indicate the robustness and optimization capability of the proposed direct HDP approaches. When the network geometry, disturbance type, or operation condition change, the conventional controller designed for a specific operating point can no longer maintain its desired performance, as in the case for the original working condition. On the other hand, the direct HDP controllers demonstrated better damping than conventional design over a wide range of system conditions because of the generalization capability of NNs.

In Case 3, the network geometry, load capacity, and system conditions had all changed. The controller, which was designed on the basis of the basic case, can no longer guarantee system stability. Therefore, it is necessary to let the weights of action and critic networks continue updating. The weight adaptation process in Case 3 is used to validate the online learning capability of the direct HDP controller under new system conditions. Figs. 6 and 7 show the performances of the direct HDP controller with fixed and continuously updated weights in Case 3.
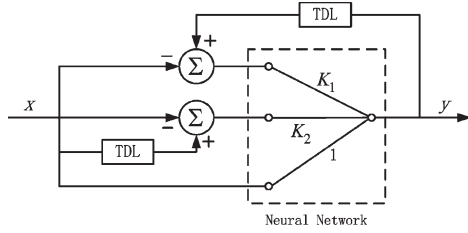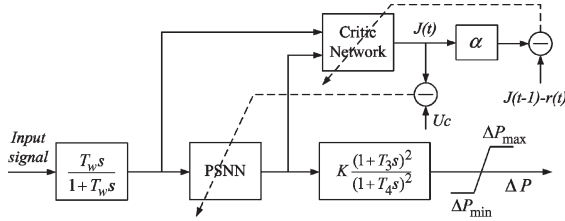
Fig. 9. Structure of PSNN.

Fig. 10. HVDC power modulation control with an embedded direct HDP controller. The action network is a PSNN.

The supplementary control using HVDC is like that, through the generator or SVC, an oscillating power control signal ΔP is produced to damp the swing.

A. Direct HDP Control in CSG

Most of the current power system stability controllers are composed of basic elements, e.g., integral, differential, inertial, and lead-lag blocks. The universal approximation capability of NNs makes it possible to replace the traditional blocks. As an example, the lead-lag block expressed in a NN structure [phase-shift neural network (PSNN)] can be derived as follows.

A lead-lag block can be described by

$$Y(s) = X(s)(1 + T_1 s)/(1 + T_2 s) \qquad (4)$$

and its discrete time realization is

$$y_{(n+1)} = x_{(n+1)} + K_1 \left(y_{(n)} - x_{(n+1)} \right) + K_2 \left(x_{(n)} - x_{(n+1)} \right) \qquad (5)$$

where $K_1 = (T_2 - \Delta t/2)/(T_2 + \Delta t/2) \backslash$ $K_2 = (\Delta t/2 - T_1)/(T_2 + \Delta t/2)$, and Δt is the discretization step size. Equation (5) can also be implemented using a neural network, as illustrated in Fig. 9, where K_1 and K_2 are the weights. This is a dynamic neural network.

Under this notion, the lead-lag block is considered implemented by an NN, and the direct HDP controller can then be embedded into traditional controllers shown in Fig. 3. Fig. 10 is the new structure used in HVDC power modulation control. The overall gain K in Fig. 10 can also be placed inside the PSNN.

The parameters other than those in the direct HDP (i.e., K, T_w, T_3, and T_4) are designed using traditional methods or based on practical experiences. The time constants in the lead-lag block must be greater than zero; consequently, K_1 and K_2 in the PSNN are also constrained. At each time step, T_1 and T_2 are calculated based on K_1 and K_2. If one of the two parameters becomes less than zero, the K values should be retained at the previous level unchanged.
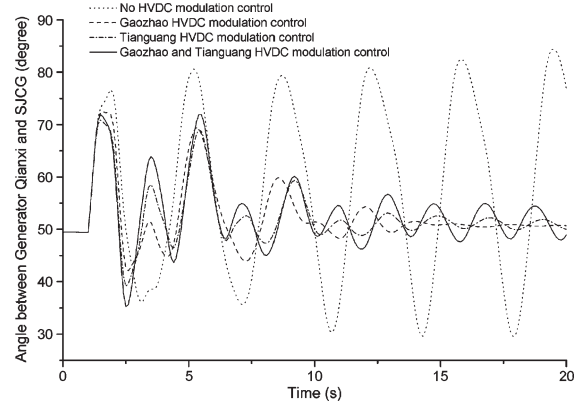

Fig. 11. Rotor angle between generator Qianxi and SJCG.

The supplementary damping controllers of the Gaozhao (Gaopo–Zhaoqing) and Tianguang (TSQ–Beijiao) HVDC links are implemented using the direct HDP controller, as shown in Fig. 10, where the input signals are chosen as the active power of the two parallel 500-kV ac lines based on the analyses of observability and dynamic relative gain array. The reinforcement signal $r(t)$ is defined as

$$r(t) = - \left(b_1 \Delta\omega_{\text{inter-1}}^2 + b_2 \Delta\omega_{\text{inter-2}}^2 \right.$$
$$\left. + b_3 \Delta\omega_{\text{local-1}}^2 + b_4 \Delta\omega_{\text{local-2}}^2 \right) \qquad (6)$$

where $\Delta\omega_{\text{inter-1}} = ((\omega_{\text{gui-1}} + \omega_{\text{gui-2}}) - (\omega_{\text{yun-1}} + \omega_{\text{yun-2}}))/2$ represents the oscillation mode between Yunan and Guizhou, $\Delta\omega_{\text{inter-2}} = ((\omega_{\text{gui-1}} + \omega_{\text{yun-1}}) - (\omega_{\text{yue-1}} + \omega_{\text{yue-2}}))/2$ represents the oscillation mode between Yunnan–Guizhou and Guangdong, and $\Delta\omega_{\text{local-1}} = \omega_{\text{yun-1}} - \omega_{\text{yun-2}}$, $\Delta\omega_{\text{local-2}} = \omega_{\text{gui-1}} - \omega_{\text{gui-2}}$ represent the local modes in Yunan and Guizhou, respectively. Therefore, most of the important modes are simultaneously considered in the cost function.

B. Coordinated Control in CSG

Since the terminals of the two dc links are not far from each other, and two more HVDC links will be in service in the coming years, the controllers must be coordinated. In Section III, the learning ability of the direct HDP was demonstrated. In this section, its coordinating design will be examined.

If only one of Gaozhao and Tianguang HVDC power modulation controllers is used, the parameters can be tuned to achieve the improved control performance after a disturbance of 40 ms short circuit on the 500-kV Huishui–Hechi ac line. However, if these independently designed controllers work together, the interactions between the two HVDC links can sometimes even deteriorate the damping capability. Fig. 11 is an illustration of reduced damping due to interactions between the HVDC links. In a multi-infeed dc system, the supplementary controllers must be designed on a coordinated basis to avoid any unexpected excitations of a new low-damped mode [15].

Since the control law update is instructed by the cost function, which is defined as the weighted sum of the squares of the relative rotor speed differences, reflecting multiple inter-province and local oscillation modes. It reflects the stability of the entire system. If only one oscillation mode is suppressed,
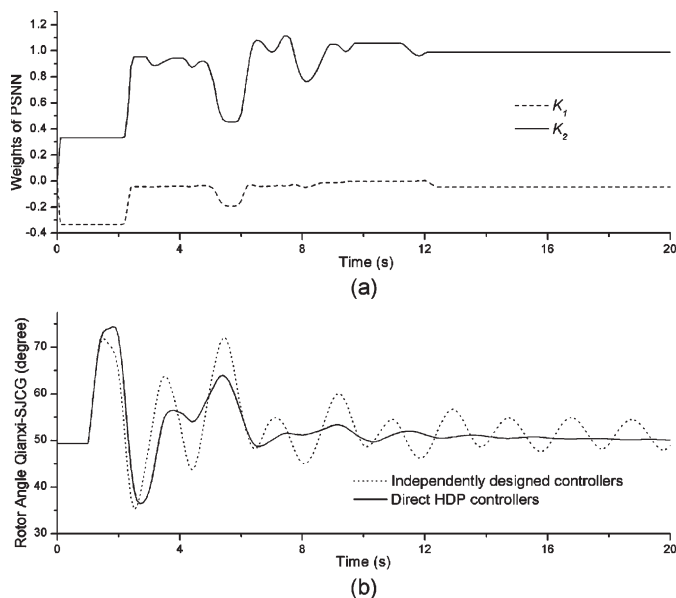
Fig. 12. Learning process and coordinated control performance.

the cost is not minimal, and the controller parameters need to be adjusted further.

Starting from the independently designed Gaozhao and Tianguang dc power modulation controllers, the new direct HDP controller can learn a set of coordinated parameters. Fig. 12(a) shows the learning process, and the variation is acceptable for real system devices.

After learning with coordination, the oscillation, including multiple modes, is properly damped, compared with the performance of the independently designed controllers, as shown in Fig. 12(b).

V. CONCLUSION

Nonlinearities, uncertainties, and the need for coordinated design are the three main problems in the stability control of a large-scale power system. In this paper, based on real system responses instead of a system model, a direct HDP controller learns to cope with model deficiencies from nonlinearities and uncertainties. Different controllers share one common cost function so that the design and adaptation are naturally coordinated. The performance of the direct HDP controller is examined through two systems. The first case is a benchmark 4M2A system, where training from random initialization and adaptations under various operating conditions demonstrate good learning abilities of the direct HDP controller. Further, integration of PSNN and coordinated learning control design are evaluated through two HVDC power modulation controllers in CSG. Superior performances over traditional control approaches are presented.

REFERENCES

[1] T. Van Cutsem and C. Vournas, *Voltage Stability of Electric Power Systems*. Boston, MA: Kluwer, 1998.
[2] D. N. Kosterev, C. W. Taylor, and W. A. Mittelstadt, "Model validation for the August 10, 1996 WSCC system outage," *IEEE Trans. Power Syst.*, vol. 14, no. 3, pp. 967–979, Aug. 1999.
[3] Q. Lu, Y. Sun, and S. Mei, *Nonlinear Control Systems and Power System Dynamics*. Boston, MA: Kluwer, 2001.
[4] J. G. Webster, *Encyclopedia of Electrical and Electronics Engineering*. New York: Wiley, 1999.
[5] K. Ohtsuka, T. Taniguchi, and T. Sato *et al.*, "A H_∞ optimal theory-based generator control system," *IEEE Trans. Energy Convers.*, vol. 7, no. 1, pp. 108–115, Mar. 1992.
[6] O. P. Malik, "Amalgamation of adaptive control and AI techniques: Applications to generator excitation control," *Annu. Rev. Control*, vol. 28, no. 1, pp. 97–106, 2004.
[7] Q. Lu, S. Mei, and W. Hu *et al.*, "Nonlinear decentralized disturbance attenuation excitation control via new recursive design for multi-machine power systems," *IEEE Trans. Power Syst.*, vol. 16, no. 4, pp. 729–736, Nov. 2001.
[8] G. K. Venayagamoorthy, R. G. Harley, and D. C. Wunsch, "Dual heuristic programming excitation neurocontrol for generators in a multimachine power system," *IEEE Trans. Ind. Appl.*, vol. 39, no. 2, pp. 282–294, Mar./Apr. 2003.
[9] D. Ernst, M. Glavic, and L. Wehenkel, "Power systems stability control: Reinforcement learning framework," *IEEE Trans. Power Syst.*, vol. 19, no. 1, pp. 427–435, Feb. 2004.
[10] J. Si and Y. T. Wang, "Online learning control by association and reinforcement," *IEEE Trans. Neural Netw.*, vol. 12, no. 2, pp. 264–276, Mar. 2001.
[11] R. Enns and J. Si, "Apache helicopter stabilization using neuro-dynamic programming," *J. Guid. Control Dyn.*, vol. 25, no. 1, pp. 19–25, 2002.
[12] R. Enns and J. Si, "Helicopter trimming and tracking control using direct neural dynamic programming," *IEEE Trans. Neural Netw.*, vol. 14, no. 4, pp. 929–939, Jul. 2003.
[13] P. Kundur, *Power System Stability and Control*. New York: McGraw-Hill, 1994.
[14] A. G. Phadke, J. S. Thorp, and M. G. Adamiak, "A new measurement technique for tracking voltage phasors, local system frequency, and rate of change of frequency," *IEEE Trans. Power App. Syst.*, vol. PAS-102, no. 5, pp. 1025–1038, May 1983.
[15] L. A. S. Pilotto, M. Szechtman, A. Wey *et al.*, "Synchronizing and damping torque modulation controllers for multi-infeed HVDC systems," *IEEE Trans. Power Del.*, vol. 10, no. 3, pp. 1505–1513, Jul. 1995.
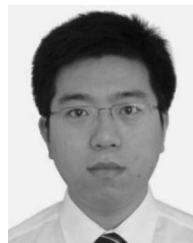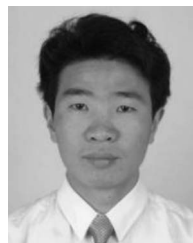
Chao Lu (M'05) received the B.E. and Ph.D. degrees from Tsinghua University, Beijing, China, in 1999 and 2005, respectively.

He is currently an Assistant Professor with the Department of Electrical Engineering, Tsinghua University. His research interests include power system analysis and control, and intelligent control applications.

Jennie Si (M'91–SM'99–F'08) received the B.S. and M.S. degrees from Tsinghua University, Beijing, China, in 1985 and 1988, and the Ph.D. degree from the University of Notre Dame, Notre Dame, IN, in 1992.

She has been with the Department of Electrical Engineering, Arizona State University, Tempe, since 1991. She became a Full Professor in 2000. Her research interests include dynamic optimization using learning and approximation methods, approximate dynamic programming solutions to large and complex systems applications, and fundamental neuroscience of cortical neural control.

Xiaorong Xie (M'02) received the B.E. degree from Shanghai Jiaotong University, Shanghai, China, in 1996, and the Ph.D. degree from Tsinghua University, Beijing, China, in 2001.

He is currently an Associate Professor with the Department of Electrical Engineering, Tsinghua University. His research interests include power system analysis and FACTS.